

Anatomy of three-body decay

III. Energy distributions

E. Garrido

*Instituto de Estructura de la Materia, CSIC, Serrano 123, E-28006 Madrid,
Spain*

D.V. Fedorov, A.S. Jensen and H.O.U. Fynbo

*Department of Physics and Astronomy, University of Aarhus, DK-8000 Aarhus
C, Denmark*

Abstract

We address the problem of calculating momentum distributions of particles emerging from the three-body decay of a many-body resonance. We show that these distributions are determined by the asymptotics of the coordinate-space complex-energy wave-function of the resonance. We use the hyperspherical adiabatic expansion method where all lengths are proportional to the hyperradius. The structures of the resonances are related to different decay mechanisms. For direct decay all inter-particle distances increase proportional to the hyperradius at intermediate and large distances. Sequential three-body decay proceeds via spatially confined quasi-stationary two-body configurations. Then two particles remain close while the third moves away. The wave function may contain mixtures which produce coherence effects at small distances, but the energy distributions can still be added incoherently. Two-neutron halos are discussed in details and illustrated by the 2^+ resonance in ${}^6\text{He}$. The dynamic evolution of the decay process is discussed.

PACS: 21.45.+v, 31.15.Ja, 25.70.Ef

1 Introduction

Nuclear resonances and excited states can be very complicated many-body structures with a number of different decay modes. The simplest decay, perhaps beside γ -emission, is breakup into two particles as exemplified by nucleon- and α -emission, and binary fission [1]. The deceptively simple breakup into

three particles is much less studied and far from understood. This is in contrast to bound three-body cluster structures where a variety of techniques are available and able to predict the properties, even of the exotic quantum halo states [2]. The three-body continuum properties are less established although rather well studied over many years [3].

Experimental information is obtained by measuring the properties of the particles in the final state. The experimental techniques are now advanced to a level where accurate and kinematically complete measurements are available on a number of different systems [4–15], and many more are expected to follow. Reliable theoretical descriptions are needed to interpret existing data, to predict unknown decay results and to help in the design of new interesting experiments. Both the structure of the initial state and the decay mechanism are essential and both must therefore be properly described simultaneously. Clearly for a genuine many-body state only the intermediate and large-distance structure is decisive. The small distance behavior is artificial and only serving to provide the proper continuous boundary conditions.

For two-body decay, like α -emission, the relative potential determines all properties. In the example of α -emission, the two-body potential can be divided into short-, intermediate- and long-distance. The short-distance part is artificially adjusted to allow the correct resonance energy and the barrier region then determines the width. At large distances where the potential has vanished the energy of the α -particle is determined by energy conservation. In two-body decay the energy distribution then only reflects the width of the initial resonance. These properties are very different for decays with more than two particles in the final state.

For three-body bound states and resonances “large distance” is less well defined. However, the corresponding structure can efficiently be computed by use of the hyperspherical adiabatic expansion method [16,17]. The wave functions are in this technique expanded on basis states related to adiabatic potentials calculated as functions of the hyperradius ρ . Then ρ provides a measure of distances for the three-body problem. The wave function is usually dominated by the component related to the lowest adiabatic potential. The small-distance part (ρ small) of both wave function and potential are only directly meaningful if the particles appearing in the final state form a genuine three-body system. Otherwise this part of the effective potential is constructed to produce the correct resonance energy and provide an appropriate boundary condition for the wave function. At intermediate distances the potential has a barrier which is decisive for the width of the resonance. At large distances the resonance wave function is characterized by outgoing waves which contain information about distributions of relative energies and possibly other quantities like spin distributions.

For three-body decay the two most obvious decay mechanisms, direct and sequential, were recently studied in a schematic model in [18]. Another schematic model is also formulated in the limit where only the Coulomb interaction is important at intermediate and large distances [19]. The detailed resonance structure at small and intermediate distances were investigated in realistic models in [20]. The large-distance properties are much more difficult to calculate accurately, because either the correct continuum three-body Coulomb wave functions are unknown, or the short-range potentials may produce an almost long-range (inverse square) effective potential at large distance. In the latter case the origin is precisely as for the Efimov effect [16,21]. The corresponding potential is most likely the lowest at large distance but not necessarily also at small distances. Thus, the resonance wave function may change structure from small to large distance. The relative energy distribution arises as the result appearing at large distance. The numerical computations are then sometimes rather tricky.

The purpose of the present paper is to establish a general method to compute relative energy distributions after decay into three particles. The short- and intermediate-distance resonance structure from [18,20] is a good starting point but we need in addition to calculate the asymptotic behavior in momentum space. The asymptotics vary for the different decay mechanisms, and the related numerical treatment is difficult when all the possibilities simultaneously have to be accounted for.

We assume that formation and decay of the resonances are independent processes. The resonance could be formed by beta-decay from a neighbouring nucleus, or a window with the relevant energies can be selected in an experimental setup where contributions from other processes also are eliminated. In section 2 we develop the theoretical formalism for resonance decay. This was previously sketched by use of the saddle point approximation [22], while we here shall instead use the Zeldovich regularization of the divergent Fourier integrals [23]. In section 3 we discuss some of the important features arising from calculation of resonance wave functions by use of the hyperspherical adiabatic expansion method combined with the complex scaling method. In section 4 we illustrate in details with realistic computations for the 2^+ -resonance in ${}^6\text{He}$. Finally, section 5 contains a brief summary and the conclusions.

2 Theoretical formulation

We assume that the system of particles has been generated in a meta-stable quantum state (a resonance) that is a generalized eigen-state of the Hamiltonian with complex energy. This is a decaying state – it describes a constant flux of particles towards infinity. Suppose we have a system of detectors at

large distances which measure the momenta of the particles emerging from this decaying state. Clearly these detectors will measure the probability distribution of particle momenta in the meta-stable state, that is the absolute square of the momentum space wave-function.

2.1 Two-body resonances

The theoretical derivation is most easily understood if we first explain the idea for simple resonance decay into a two-body system. We need resonance inventions in coordinate and momentum-space and transformations between these non-square integrable functions.

2.1.1 Resonance wave functions

The momentum space wave-function of a resonant state with the complex energy $E_r = \frac{\hbar^2}{2m} k_0^2 = E_0 - i\frac{\Gamma}{2}$ has the form [24]

$$\psi_{k_0}(\mathbf{k}) = \frac{g(k, \Omega_k)}{k^2 - k_0^2}, \quad (1)$$

where \mathbf{k} is the relative momentum and Ω_k indicates the two angles defining the direction of the vector \mathbf{k} . We assume that the wave function $\psi_{k_0}(\mathbf{k})$ only has the pole at $k = k_0$ and $g(k, \Omega_k)$ is then a continuous function of the momentum \mathbf{k} with no poles.

The distribution $P(\mathbf{k})$ of the relative momentum \mathbf{k} of the two particles in the resonant state ψ_{k_0} is given by the absolute square of the momentum-space wave function, i.e.

$$P(\mathbf{k}) = |\psi_{k_0}(\mathbf{k})|^2 \propto \frac{|g(k, \Omega_k)|^2}{(E - E_0)^2 + \frac{\Gamma^2}{4}}, \quad (2)$$

where the real observable energy E is $E = \hbar^2 k^2 / (2m)$. The approximation that the system is generated in a pure resonant state ψ_{k_0} is most likely only valid in the neighborhood of the resonant energy, i.e. $E \simeq E_0$. Furthermore, the function $g(k, \Omega_k)$ is smooth and varies by definition much less than the denominator in eq.(1). In any case we shall only consider energies where $|E - E_0|$ is less than a few times Γ . We can then confidently substitute the momentum k with the resonant momentum k_0 in $g(k, \Omega_k)$ and thus arrive at the expression

of the famous Breit-Wigner type

$$P(\mathbf{k}) \propto \frac{|g(k_0, \Omega_k)|^2}{(E - E_0)^2 + \frac{\Gamma^2}{4}}, \quad (3)$$

where the energy dependence is given by the factor $[(E - E_0)^2 + \frac{\Gamma^2}{4}]^{-1}$ while the angular dependence is given by the (absolute square of the) function $g(k_0, \Omega_k)$. Thus, the momentum-space wave-function eq.(1) of the resonance allows direct calculation of the momentum distributions of the decay fragments through eq.(3). Clearly improvements are possible by use of different approximations of $g(k, \Omega_k)$.

Instead of momentum-space, the wave-function of the resonance may be available in coordinate-space where the large-distance asymptotic form is given by

$$\psi_{k_0}(\mathbf{r}) \xrightarrow{r \rightarrow \infty} \frac{e^{+ik_0r}}{r} f(\Omega_r), \quad (4)$$

where Ω_r denotes the two angles defining the direction of the relative coordinate \mathbf{r} . The structure is an outgoing spherical wave potentially modified by an angular dependence contained in $f(\Omega_r)$. Generally the resonance wave function can be written as a partial-wave expansion in the spherical harmonics Y_{lm} , i.e.

$$\psi_{k_0}(\mathbf{r}) = \sum_{lm} C_{lm} \chi_l(r) Y_{lm}(\Omega_r), \quad (5)$$

where C_{lm} are constants depending on angular momentum and projection quantum numbers l and m . The radial functions $\chi_l(r)$ are those solutions of the radial Schrödinger equation that asymptotically approach the outgoing spherical wave in eq.(4), i.e.

$$\chi_l(r) \xrightarrow{r \rightarrow \infty} \frac{e^{+ik_0r}}{r}, \quad f(\Omega_r) = \sum_{lm} C_{lm} Y_{lm}(\Omega_r). \quad (6)$$

This defines the asymptotic behavior of the decaying resonance wave function which in turn determines the energy distribution in the observable final state.

2.1.2 Transformation from coordinate- to momentum-space

The coordinate-, $\psi_{k_0}(\mathbf{r})$, and momentum-space, $\psi_{k_0}(\mathbf{k})$, wave-functions are connected via a Fourier transform

$$\psi_{k_0}(\mathbf{k}) = \int e^{-i\mathbf{k}\mathbf{r}} \psi_{k_0}(\mathbf{r}) d^3r. \quad (7)$$

Expansion of the plane-wave in terms of spherical harmonics

$$e^{i\mathbf{k}\mathbf{r}} = \sum_{lm} 4\pi i^l j_l(kr) Y_{lm}(\Omega_r) Y_{lm}^*(\Omega_k) \quad (8)$$

reduces the Fourier integral in eq.(7) to a one-dimensional radial integral

$$\psi_{k_0}(\mathbf{k}) = 4\pi \sum_{lm} C_{lm} (-i)^l Y_{lm}(\Omega_k) \int_0^\infty r^2 dr \chi_l(r) j_l(kr). \quad (9)$$

Because of the asymptotics in eq.(6) the radial integral is seen to diverge. The large-distance behavior is responsible for the divergence. The physics content, expressed by a finite value, then has to be extracted by a suitable regularization. We use the prescription proposed by Zeldovich [23], i.e. multiplication of the integrand by a gaussian where the range after integration is increased to infinity. For an exponential this gives

$$\int_0^\infty e^{iqr} dr \rightarrow \lim_{\alpha \rightarrow 0} \int_0^\infty e^{iqr - \alpha^2 r^2} dr = \lim_{\alpha \rightarrow 0} e^{-\frac{q^2}{4\alpha^2}} \frac{\sqrt{\pi}}{2\alpha} \operatorname{erfc}\left(-\frac{iq}{2\alpha}\right) = \frac{i}{q}, \quad (10)$$

where q can be complex and erfc is the error function of complex argument. In the present context the radial integral in eq.(9) is first rewritten by adding and subtracting the asymptotic expression of the diverging integrand. The difference between the true and the asymptotic expression then remains finite even without multiplication by the gaussian function. Only the asymptotic expression then diverges when the gaussian smoothly converges to an overall factor of one.

The physics content is extracted by dividing with a similarly diverging normalization integral of the square of the wave function $\chi_l(r)$. Also this integral, now in the denominator, is rewritten by addition and subtraction of its asymptotic expression. Again only the asymptotic expression diverges. The Zeldovich prescription now leaves the ratio of these two diverging integrals of the asymptotic expressions. However, this ratio does not diverge but converge towards the physically meaningful result. Apart from a normalization we therefore have

to regularize only the asymptotic expression obtained by use of eq.(6) and the asymptotic approximation of $j_l(kr)$, i.e.

$$\psi_{k_0}(\mathbf{k}) = 4\pi \sum_{lm} C_{lm} (-i)^l Y_{lm}(\Omega_k) \int_0^\infty r^2 dr \frac{e^{+ik_0r}}{r} \frac{\sin(kr - \frac{l\pi}{2})}{kr}. \quad (11)$$

The radial integral is then by use of eq.(10) evaluated to be

$$\begin{aligned} \int_0^\infty e^{+ik_0r} \sin(kr - \frac{l\pi}{2}) dr &= \frac{i^l}{2} \left[\frac{1}{k - k_0} - \frac{(-1)^l}{k + k_0} \right] \\ &= \frac{i^l k + k_0 - (-1)^l (k - k_0)}{2(k^2 - k_0^2)} = i^l \frac{k_0}{k^2 - k_0^2} \quad \text{or} \quad i^l \frac{k}{k^2 - k_0^2} \end{aligned} \quad (12)$$

for even or odd l , respectively. The summation in eq.(11) is proportional to the angular amplitude f from eq.(6), but now as a function of the momentum \mathbf{k} . In any case we assumed earlier that $k \approx k_0$ in the smooth functions. We therefore arrive at the final expression for the Fourier-transform of the resonance wave-function, i.e.

$$\psi_{k_0}(\mathbf{k}) = \frac{4\pi}{k^2 - k_0^2} \sum_{lm} C_{lm} Y_{lm}(\Omega_k) = \frac{4\pi}{k^2 - k_0^2} f(\Omega_k). \quad (13)$$

Thus the function g from eq.(1) is then related to f from eq.(4) by

$$g(k_0, \Omega_k) = 4\pi f(\Omega_k). \quad (14)$$

The convenient fact that only the asymptotic limit of the resonance wave function enters after the regularization procedure is perhaps more surprising in mathematics than in physics where the observable energy distributions always are obtained from the properties at large distances.

The observable distribution in momentum-space is determined by the angular wave function in coordinate-space evaluated for angles describing the direction of the momentum. This peculiar fact can intuitively be understood by the geometry of particles moving towards the detectors at infinitely large distances. Coordinates and momenta then must point in the same direction. A mathematical formulation is available from ionization cross sections calculated for atomic physics processes [25].

2.2 Three-body resonances

The generalization to three particles first requires a convenient set of coordinates. We choose the scaled Jacobi coordinates [16]

$$\begin{aligned}\mathbf{x} &= \sqrt{\frac{m_2 m_3}{m(m_2 + m_3)}} (\mathbf{r}_2 - \mathbf{r}_3), \\ \mathbf{y} &= \sqrt{\frac{m_1(m_2 + m_3)}{m(m_1 + m_2 + m_3)}} \left(\mathbf{r}_1 - \frac{m_2 \mathbf{r}_2 + m_3 \mathbf{r}_3}{m_2 + m_3} \right),\end{aligned}\tag{15}$$

where m is a mass scale, and \mathbf{r}_i and m_i are the coordinate and mass of the particle number i . The hyper-spherical coordinates are then the hyper-radius ρ , the hyper-angle α , and the directional angles Ω_x and Ω_y of the vectors \mathbf{x} and \mathbf{y} defined by

$$\rho = \sqrt{x^2 + y^2} \quad , \quad \alpha = \arctan(x/y) \quad , \quad \Omega_\rho = \{\alpha, \Omega_x, \Omega_y\} .\tag{16}$$

The Jacobi coordinates depend on the sequence chosen for the particles, and the three different pairs of \mathbf{x} and \mathbf{y} could be labeled to distinguish. We omit these labels when the meaning is clear.

The corresponding momentum-space variables are

$$\kappa = \sqrt{p^2 + q^2} \quad , \quad \alpha_\kappa = \arctan(q/p) \quad , \quad \Omega_\kappa = \{\alpha, \Omega_p, \Omega_q\} ,\tag{17}$$

where \mathbf{p} and \mathbf{q} are the conjugate momenta related to the coordinates \mathbf{x} and \mathbf{y} .

2.2.1 No bound two-body subsystems

The generalization of the two-body spherical harmonics are the so-called hyper-spherical harmonics [16]

$$\begin{aligned}\mathcal{Y}_{\mathcal{K}}(\Omega_\rho) &= N_n^{(l_x, l_y)} \sin^{l_x} \alpha \cos^{l_y} \alpha P_n^{(l_x + \frac{1}{2}, l_y + \frac{1}{2})}(\cos 2\alpha) \\ &\quad \times Y_{l_x m_x}(\Omega_x) Y_{l_y m_y}(\Omega_y)\end{aligned}\tag{18}$$

where $\mathcal{K} \equiv \{K l_x m_x l_y m_y\}$, $K = 2n + l_x + l_y$, and (l_x, m_x, l_y, m_y) are the angular quantum numbers related to coordinates \mathbf{x} and \mathbf{y} , and $N_n^{(l_x, l_y)}$ is a normalization factor. These functions are the eigen-functions of the angular part Λ^2 of

the three-body kinetic energy operator T

$$T = \frac{\hbar^2}{2m}(\nabla_x^2 + \nabla_y^2) = \frac{\hbar^2}{2m} \left[-\frac{\partial^2}{\partial \rho^2} - \frac{5}{\rho} \frac{\partial}{\partial \rho} + \frac{\Lambda^2}{\rho^2} \right] \quad (19)$$

with the eigenvalues $K(K+4)$, i.e.

$$\Lambda^2 \mathcal{Y}_K(\Omega_\rho) = K(K+4) \mathcal{Y}_K(\Omega_\rho), \quad (20)$$

where K is a non-negative integer. Without Coulomb and without bound two-body subsystems the three-body resonance wave-function $\Psi_{\kappa_0}(\rho, \Omega_\rho)$ with the complex energy $E_r = \hbar^2 \kappa_0^2 / (2m) = E_0 - i\Gamma_0/2$ can be expanded in terms of the hyper-spherical harmonics

$$\Psi_{\kappa_0}(\rho, \Omega_\rho) = \sum_{\mathcal{K}} C_{\mathcal{K}} \chi_{\mathcal{K}}(\rho) \mathcal{Y}_{\mathcal{K}}(\Omega_\rho), \quad (21)$$

where the hyper-radial functions $\chi_{\mathcal{K}}(\rho)$ have the usual resonance asymptotic behavior of an out-going hyper-spherical wave

$$\chi_{\mathcal{K}}(\rho) \xrightarrow{\rho \rightarrow \infty} \frac{e^{+i\kappa_0 \rho}}{\rho^{5/2}}. \quad (22)$$

The three-body wave-function asymptotically has the form of the hyper-spherical wave with an angular amplitude $F(\Omega_\rho)$ determined by the expansion coefficients $C_{\mathcal{K}}$, i.e.

$$\Psi_{\kappa_0}(\rho, \Omega_\rho) \xrightarrow{\rho \rightarrow \infty} \frac{e^{+i\kappa_0 \rho}}{\rho^{5/2}} \sum_{\mathcal{K}} C_{\mathcal{K}} \mathcal{Y}_{\mathcal{K}}(\Omega_\rho) \equiv \frac{e^{+i\kappa_0 \rho}}{\rho^{5/2}} F(\Omega_\rho). \quad (23)$$

The momentum-space wave-function is the Fourier transform

$$\Psi_{\kappa_0}(\kappa, \Omega_\kappa) = \int e^{-i\mathbf{p}\mathbf{x} - i\mathbf{q}\mathbf{y}} \Psi_{\kappa_0}(\rho, \Omega_\rho) \rho^5 d\rho d\Omega_\rho. \quad (24)$$

The three-body plane-wave can be expanded in hyper-spherical harmonics as

$$e^{i\mathbf{p}\mathbf{x} + i\mathbf{q}\mathbf{y}} = \frac{(2\pi)^3}{(\kappa\rho)^2} \sum_{\mathcal{K}} i^K J_{K+2}(\kappa\rho) \mathcal{Y}_{\mathcal{K}}(\Omega_\rho) \mathcal{Y}_{\mathcal{K}}^*(\Omega_\kappa). \quad (25)$$

Due to orthogonality of the hyper-spherical harmonics the angular part of the integral in eq.(24) is trivial and we are only left with the hyper-radial integral

$$\Psi_{\kappa_0}(\kappa, \Omega_\kappa) = \frac{(2\pi)^3}{\kappa^2} \sum_{\mathcal{K}} (-i)^K C_{\mathcal{K}} \mathcal{Y}_{\mathcal{K}}(\Omega_\kappa) \int \rho^3 d\rho \chi_{\mathcal{K}}(\rho) J_{K+2}(\kappa\rho). \quad (26)$$

Precisely as in the two-body case, in the vicinity of the resonance the integrand can be made ready for regularization by substitution of eq.(22) and the asymptotic form

$$J_{K+2}(\kappa\rho) \xrightarrow{\rho \rightarrow \infty} -\sqrt{\frac{2}{\pi\kappa\rho}} \sin(\kappa\rho - \frac{\pi K}{2}). \quad (27)$$

This results in a diverging integral similar to that of the two-body case

$$\Psi_{\kappa_0}(\kappa, \Omega_\kappa) = -\frac{(2\pi)^3}{\kappa^{5/2}} \sqrt{\frac{2}{\pi}} \sum_{\mathcal{K}} (-i)^K C_{\mathcal{K}} \mathcal{Y}_{\mathcal{K}}(\Omega_\kappa) \int d\rho e^{+i\kappa_0\rho} \sin(\kappa\rho - \frac{\pi K}{2}). \quad (28)$$

Using the Zeldovich regularization leads to

$$\begin{aligned} \Psi_{\kappa_0}(\kappa, \Omega_\kappa) &= -\frac{(2\pi)^3}{\kappa_0^{5/2}} \sqrt{\frac{2}{\pi}} \sum_{\mathcal{K}} (-i)^K C_{\mathcal{K}} \mathcal{Y}_{\mathcal{K}}(\Omega_\kappa) \frac{i^K}{2} \frac{2\kappa_0}{\kappa^2 - \kappa_0^2} \\ &= -\frac{2^{7/2} \pi^{5/2}}{\kappa_0^{3/2}} \frac{1}{\kappa^2 - \kappa_0^2} F(\Omega_\kappa), \end{aligned} \quad (29)$$

that is, in the vicinity of the resonance, the angular wave function in momentum-space is proportional to that in coordinate-space but evaluated for the momentum variables. The energy distribution is determined by the Breit-Wigner factor where the width is obtained from the three-body resonance. The function $F(\Omega_\kappa)$ now contains information about the non-trivial energy distribution between the three particles. This is in contrast to the two-body decay where all the energy is in the only existing relative degree of freedom.

2.2.2 One bound two-body subsystem

Sometimes a bound two-body subsystem can be emitted from a three-body resonance. Such a final state configuration can not be described by hyper-spherical harmonics. However if this is the only open channel, the description of such a decay reduces to the two-body case. Indeed the asymptotics of the resonance wave-function is then

$$\Psi_{\kappa_0}(\rho, \Omega_\rho) \xrightarrow{\rho \rightarrow \infty} \phi_{23}(\mathbf{x}) \frac{e^{iq_0 y}}{y} f(\Omega_y), \quad (30)$$

where $\phi_{23}(\mathbf{x})$ describes a bound system of particles 2 and 3 with binding energy B_{23} , $q_0 = \sqrt{2m(E_r - B_{23})/\hbar^2}$, $f(\Omega_y)$ is the angular amplitude and E_r is the complex three-body energy. If both three-body and two-body decays are possible the wave-function contains asymptotics of both two- and three-body types,

$$\Psi_{\kappa_0}(\rho, \Omega_\rho) \xrightarrow{\rho \rightarrow \infty} A \frac{e^{+i\kappa_0\rho}}{\rho^{5/2}} F(\Omega_\rho) + B \phi_{23}(\mathbf{x}) \frac{e^{iq_0 y}}{y} f(\Omega_y), \quad (31)$$

where A and B are the asymptotic coefficients determining the relative weights of the two decay channels. Both F and f are dimensionless and the dimension (length to $-3/2$) of ϕ_{23} compensate for the one length in the denominator of the last term.

The Fourier transform and the corresponding regularization then give the momentum-space wave function, i.e.

$$\Psi_{\kappa_0}(\kappa, \Omega_\kappa) = -\frac{2^{7/2}\pi^{5/2}}{\kappa_0^{3/2}} \frac{A}{\kappa^2 - \kappa_0^2} F(\Omega_\kappa) + B \phi_{23}(\mathbf{p}) \frac{4\pi}{q^2 - q_0^2} f_y(\Omega_q), \quad (32)$$

where $q^2 = \kappa^2 - 2mB_{23}/\hbar^2$, $\phi_{23}(\mathbf{p})$ is the momentum-space wave function of the two-body bound state ϕ_{23} . These two channels correspond, respectively, to two close-lying particles in a bound state far away from the third one, and three particles all far away from each other. Thus, in the of large distances they do not interfere, and the resulting momentum distribution is simply a weighted sum of the corresponding distributions. The relative contributions of the two channels are given by $|A|^2$ and $|B|^2$ correspondingly.

Generalization to describe decays into more than one two-body bound state is formally straightforward, i.e. the corresponding non-interfering asymptotic terms should simply be added. This holds for more than one bound state in the same two-body system as well as for bound states in different two-body systems.

2.2.3 One resonant two-body subsystem

Instead of a bound state the decay via a two-body resonance is often considered in interpretation and analysis of experiments. Clearly the narrower the resonance the more similarity to the case of two-body bound states. In any case the hyper-spherical expansion must eventually converge, although the convergence can be too slow for a reliable extraction of the asymptotic coefficients in eq.(23) from a numerical solution of the three-body problem.

However, in this case the (slowly convergent) two-body resonance configuration can then be explicitly included into the asymptotics while only the remaining (hopefully fast convergent) part is expanded, i.e.

$$\Psi_{\kappa_0}(\rho, \Omega_\rho) \xrightarrow{\rho \rightarrow \infty} A \frac{e^{+i\kappa_0\rho}}{\rho^{5/2}} F(\Omega_\rho) + B \frac{e^{ip_0x}}{x} f_x(\Omega_x) \frac{e^{iq_0y}}{y} f_y(\Omega_y), \quad (33)$$

where $\hbar^2\kappa_0^2/(2m) = E_0 - i\Gamma_0/2$ is the complex three-body energy, $\hbar^2p_0^2/(2m) = E_{23}^{(0)} - i\Gamma_{23}/2$ is the (complex) energy of the two-body resonance and the remaining part is described by the complex momentum $q_0^2 = \kappa_0^2 - p^2$. The precise definition of q_0^2 arises from a constraint to be seen below.

The corresponding momentum-space wave-function is again given by the regularized Fourier transform, i.e.

$$\Psi_{\kappa_0}(\kappa, \Omega_\kappa) = -A \frac{2^{7/2}\pi^{5/2}}{\kappa_0^{3/2}} \frac{F(\Omega_\kappa)}{\kappa^2 - \kappa_0^2} + B \frac{4\pi}{p^2 - p_0^2} f_x(\Omega_p) \frac{4\pi}{q^2 - q_0^2} f_y(\Omega_q). \quad (34)$$

The momentum distribution is given by the absolute square of this momentum-space wave-function. In the center of mass system we can directly find the distribution of particle 3 arising from the sequential emission via the two-body resonance.

Absolute square of the last term in eq.(34) and use of the energy conservation $\kappa^2 = q^2 + p^2$ (or $E = E_1 + E_{23}$) immediately gives the energy distribution for particle 1

$$P(E_1) \propto \int dE_{23} \frac{1}{[(E_{23} - E_{23}^{(0)})^2 + \Gamma_{23}^2/4]} \frac{1}{[(E_{23} + E_1 - E_0)^2 + \Gamma_0^2/4]} \\ \propto \frac{1}{(E_1 - (E_0 - E_{23}^{(0)}))^2 + (\Gamma_0 + \Gamma_{23})^2/4}, \quad (35)$$

which states that the most probable energy of particle 1 is $E_1 = E_0 - E_{23}^{(0)}$ and the width of the distribution is the sum of the two and the three-body widths. Precisely this Breit-Wigner distribution only arises when the $|q^2 - q_0^2|^2$ in eq.(34) is proportional to $(E - E_0)^2 + \Gamma_0^2/2$, i.e. given by the probability distribution in the initial three-body state, which also is of Breit-Wigner form. Thus the definition of q_0^2 must involve p^2 and not p_0^2 .

The same integration could of course be performed on the energy of particle 1, but this would only give the two-body Breit-Wigner distribution for E_{23} whereas the measurements provide individual energies, E_2 and E_3 , for particles 2 and 3 in the center of mass system. To get the distributions of E_2 and E_3

involve trivial but tedious kinematical transformations where also energies and directions of particle 1 are required.

2.2.4 *Alternative real-coordinate procedure*

The relative energy distributions can be obtained from the angular resonance wave function calculated without complex scaling. We assume that the system of particles is produced in an initial state for example by a beta-decay process. We can then imagine the subsequent decay as the time evolution of the initial non-stationary state. This can be formulated as a time dependent coupled channels problem. It can also be viewed intuitively as a particle described by time dependent coordinates determined by classical equations of motion. This should be done with the appropriate initial amplitudes for all parts of the initial wave function. The hyperradius must vary from being very small to infinitely large. We increase ρ until all particles are outside the interaction ranges of all other particles. From then on all distances scale as ρ and all other coordinates remain unchanged with time until $\rho = \infty$.

Energy conservation is maintained at large distances by converting the potential energy into kinetic energy in the scaling degree of freedom, i.e. by increasing the velocity $\dot{\rho}$ of the ρ -coordinate. The wave function then evolves with all angular degrees of freedom frozen eventually reaching the detectors placed far away. The absolute square of the angular wave function as function of $\cos^2 \alpha$ then provide the energy distributions simply because the kinetic energy of particle 1 is given by the velocity of y , i.e. $\dot{y} = \dot{\rho} \cos \alpha$. Then the energy distribution as function of the kinetic energy, proportional to $\dot{y}^2 \propto \cos^2 \alpha$, is the probability coordinate-space distribution as function of $\cos^2 \alpha$, apart from the phase space conversion from α to energy, i.e. division by a factor proportional to $dE/d\alpha \propto \sin(2\alpha)$.

This procedure is tempting since we only need to increase the maximum value of ρ in all the numerical implementations and plot the wave function at that large distance. For this to be accurate the asymptotics has to be well described by the hyperspherical expansion or the basis has to be very large and able to describe the necessary large ρ -behavior. However, when the basis functions have asymptotics different from one of the intermediate structures the size of the basis needed to reach convergence can easily become huge, making the procedure impractical. This is not necessarily easy to see in the numerical results where an increase of basis size usually is rather expensive while the convergence could be extremely slow. The procedure is probably only directly useful for direct decay or for sequential decay via broad resonances. Otherwise the different intermediate structure should be computed somehow and extrapolations to large distances applied to each component individually.

An example to illustrate the present alternative formulation is available in the schematic model discussed in details in [18] where the widths but not the energy distribution were computed. Assume that only the Coulomb potential is important and the most probable path (ridge in the wave function) from small to large distances can be described by scaling the hyperradius. The corresponding optimum path is defined by minimizing the WKB-tunneling expression as function of different relative scaling parameters $s_{ik} = r_{ik}/\rho$, where r_{ik} is the distance between particles i and k . The path is given by $s_{ik}^3 m_i Z_j = s_{jk}^3 m_j Z_i$ (see also [19]), where $Z_i e$ is the charge of particle i . We then arrive at the most probable value for the energy division, i.e.

$$E_k = E_{total} \left(1 + \left(\frac{m_k Z_k^2}{m_i Z_i^2} \right)^{1/3} + \left(\frac{m_k Z_k^2}{m_j Z_j^2} \right)^{1/3} \right)^{-1}, \quad (36)$$

where E_{total} is the total energy distributed among all the three particles. This expression is simple but not very accurate. It also only provides an estimate of the peak value. To compute the distribution other paths must also be considered. This is possible but we shall leave this for a later discussion in connection with a detailed treatment of the Coulomb interaction.

3 Resonance wave functions

The resonance wave function contains all information including that of the relative energy distribution after the decay. The calculations must then first provide the corresponding three-body resonance states. Second the large-distance behavior must be accurately extracted. Due to the different structures, these steps are not trivially completed by use of only one method. We briefly describe first the main ingredients in our computations and the features of the wave function. Second we explain how the asymptotic behavior is obtained in practice.

3.1 Method

We use the hyperspherical adiabatic expansion method combined with complex scaling to obtain resonance wave functions. The coordinates are defined in section 2 along with our basis functions in angular space, i.e. the hyperspherical harmonics in each of the three Jacobi systems. We solve the complex scaled Faddeev equations as function of hyperradius [16,26]. The complex scaled coupled set of radial equations are subsequently solved with the appropriate boundary conditions, i.e. exponentially vanishing with increasing ρ for

both bound states and resonances. Thus here we assume that we do not need to treat the Coulomb interaction explicitly at asymptotic large distances. As shown in [26], the results obtained with this method agree well with some of the most common procedures, as for instance the complex energy method.

The energies are usually accurately determined in this method. The same applies to the wave functions at small and intermediate distances where the exponential fall-off still is not too restrictive. However, we need the information at distances where the asymptotic limit is reached, i.e. possibly at very large ρ where the complex scaled wave functions are very small. Furthermore, more than one geometric structure can be important at the same time, e.g. two different spatially confined two-body configurations with the (different) third particle far away. This happens frequently with two identical particles like neutrons and protons as constituent particles, because the nucleon-core interaction must be sufficiently attractive to produce a bound or resonating three-body system, and this implies that such two-body configurations are favored. To account simultaneously for different two-body substructures, it is essential to use three components as in the Faddeev decomposition adopted by us. The same efficiency can be achieved in a variational approach by allowing Faddeev-like components in the trial wave function [27]. It is much more difficult, if not impossible, to reach convergence with only one component as in the hyperharmonic expansion method [28].

Even with three Faddeev components a large basis has to be employed. To describe substructures inside one of the two-body potentials (range R_{eff}) for large ρ we need values of the hyperpshpherical quantum number K up to a few times $\rho\sqrt{m}/(R_{eff}\sqrt{\mu})$ where μ is the reduced mass of the two particles. This is because $K/2$ is the number of nodes in the basis, and details can only be described if a few nodes can be placed inside the structure in question. Thus, for nuclear systems, where $R_{eff} \simeq 4$ fm, we need K_{max} of at least 50 to describe such structures for $\rho \simeq 100$ fm. Employing complex scaling transforms resonances into states obeying the numerically easier bound state boundary conditions. The required basis size is larger, essentially because the exponential fall-off moves to larger distances with increasing scaling angle. These estimates provide necessary conditions for a reasonable description of two-body substructures which in turn are necessary to describe the sequential decay mechanism.

The requirement of large K to describe substructures must be reconciled with the fact that an increase of ρ towards infinity results in convergence of the angular eigenvalues to the hyperharmonic spectrum for free particles. We show an example in Fig. 1 where the imaginary parts are omitted as they both oscillate around zero and approach zero at large ρ . The real parts of the angular eigenvalues approach $K(K + 4)$ as ρ increases while the corresponding potentials all approach zero faster than ρ^{-2} . The attractive pockets in the

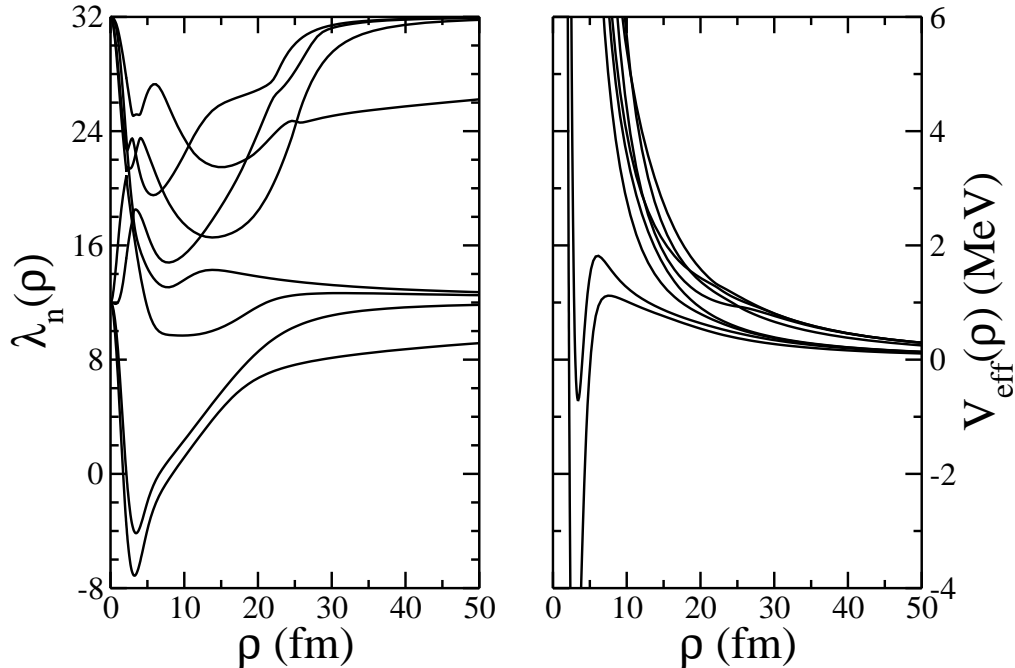


Fig. 1. The real parts of the lowest 8 angular eigenvalues (left) and corresponding adiabatic potentials (right) as functions of ρ for the 2^+ states in ${}^6\text{He}$ (${}^4\text{He} + n + n$). The scaling angle is $\theta = 0.10$ rads.

eigenvalues at short distance disappear in the potentials except for the two lowest where the negative values remain as a prominent feature. The approach to the asymptotic values is very fast except for the levels where s -waves contribute significantly. The low energies favor these levels at large distances.

The related adiabatic wave functions approach the hyperspherical harmonics. The reason is that the regions in space, where the short-range interactions are significant, are shrinking in size with increasing ρ relative to the total space available. The radial extension of these regions, responsible for two-body correlations, decrease with ρ as $1/\rho$. The interactions are non-vanishing in smaller and smaller regions. Consequently they become less and less important for both energies and wave functions. Thus, the basis size has to increase with ρ in order to allow a description of the two-body substructures or equivalently of sequential decay, but the lowest adiabatic potentials approach the free solutions. The basis size in practice always has to remain finite and the substructures eventually become impossible to describe in this way.

The interactions have to be chosen to reproduce the pairwise low-energy scattering properties of the three particles appearing in the final state. Clearly we must accurately include all the partial waves necessary to describe the quantum numbers of the decaying resonance. However, even with a sufficiently

large basis the three-body system does not necessarily appear with the correct energy and width. In fact, there may not even be an attractive region at small distances as required to produce a resonance of finite width. This could occur when we are dealing with a many-body resonance without traces of any three-body cluster structure. Nevertheless, a meaningful computation can be carried out of the energy distributions emerging after a three-body decay.

The philosophy is the same as for α -emission where the inner part of the effective potential is replaced by an attractive square well with a depth adjusted to reproduce the resonance energy. The resulting barrier is then used to derive the width, usually in the WKB approximation. We generalize this concept to the adiabatic potentials, i.e. we add a three-body potential of short range in the hyperradius. It is intended to describe interactions beyond the two-body level such that the three-body system has a resonance at the desired energy. By doing this we have substituted the possibly complicated many-body structure at small distance with the three-body cluster structure resulting from an effective potential, which in turn also provides the correct boundary conditions for a three-body decaying resonance. This principle was introduced for fine-tuning in the first calculation with the correct boundary conditions of the three- α decay of the second 0^+ -state in ^{12}C [29]. It has later become the standard procedure to adjust three-body energies without significant changes of the underlying substructure [16].

3.2 *Important features*

The radial solution is often strongly dominated by one or two of the lowest adiabatic components at small distance where the relative probability is large. This is because all three short-range two-body interactions contribute simultaneously and the result is the energetically most favored three-body resonance structure consistent with the boundary conditions. As ρ increases, at least one particle has to move away from the other leaving at most one non-vanishing two-body interaction. Coherent contributions from different of these configurations are possible and sometimes even favored. At large distance, where the energy distribution is determined, several more adiabatic potentials are often needed. The couplings due to the Coulomb interaction would normally increase the necessary number of potentials.

It is established [16] that the adiabatic potentials of lowest energy at large ρ are related to configurations with relative s -waves between the two closest particles. This is the basis for the Efimov effect [30]. If these large-distance configurations differ from the resonance structure at small ρ , possibly with higher partial waves, the lowest angular wave function must change its structure accordingly as ρ increases. In [20] we showed the structure for $^6\text{He}(2^+)$ for the

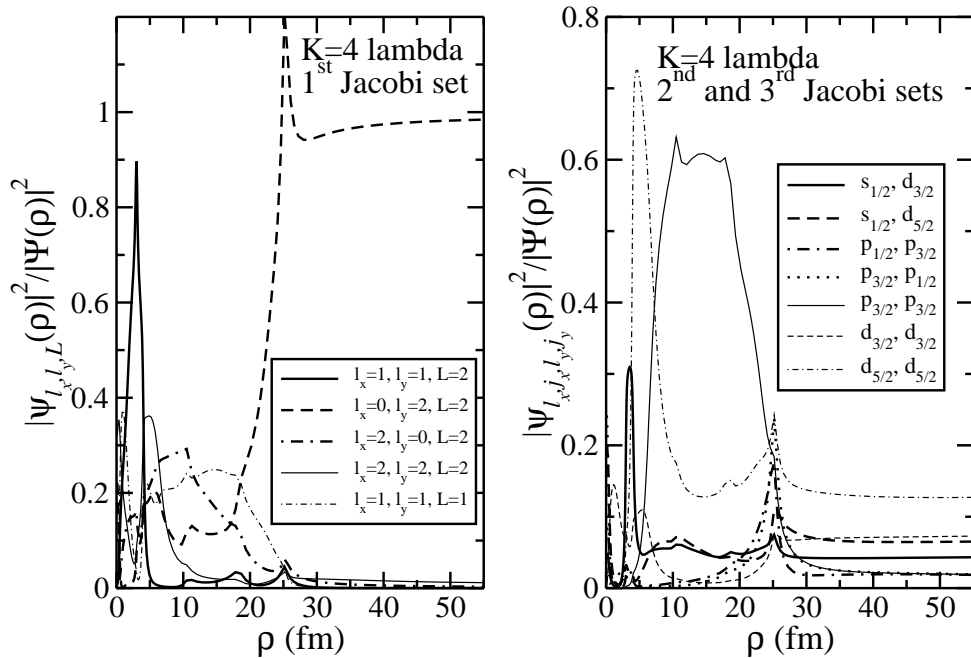


Fig. 2. The fraction of different components in the fifth adiabatic potential for $\theta = 0.10$ rads as function of ρ for ${}^6\text{He}(2^+)$. The angular eigenvalue corresponds to $K = 4$ at large ρ , see Fig. 1. The angular momenta are specified by ℓ_x, j_x, ℓ_y, j_y , and L . Left: x refers to the two-neutron system and y to its center of mass motion relative to the α -particle. Right: x refers to the neutron- α system and y to its center of mass motion relative to the other neutron. We give the (x, y) components on the figure as ℓ_j .

lowest eigenvalue which approach the $K = 2$ value at large ρ . In Fig. 2 we show the results for the similar eigenvalue approaching the $K = 4$ level for large ρ . The pronounced and rapidly changing structure is qualitatively similar to the lower-lying $K = 2$ level, i.e. dominated by $p_{3/2} - p_{3/2}$ neutron-core structure at small ρ and by s -waves between the two neutrons at large ρ . Essentially all other allowed components contribute with equally small amounts.

These rather dramatic changes imply that it is crucial to include all adiabatic potentials with significant couplings to those dominating the structure at small hyperradii. This is simply because the couplings are responsible for changing the radial weights of the different adiabatic components as function of ρ , e.g. no couplings imply the same occupation independent of ρ . On the other hand, each of the angular wave functions related to the adiabatic potentials are themselves functions of ρ , sometimes rapidly varying as seen in Fig. 2. In principle the non-diagonal couplings could be vanishingly small and all change of structure would be described by the lowest adiabatic wave function. However, this is rather unlikely because the couplings are defined

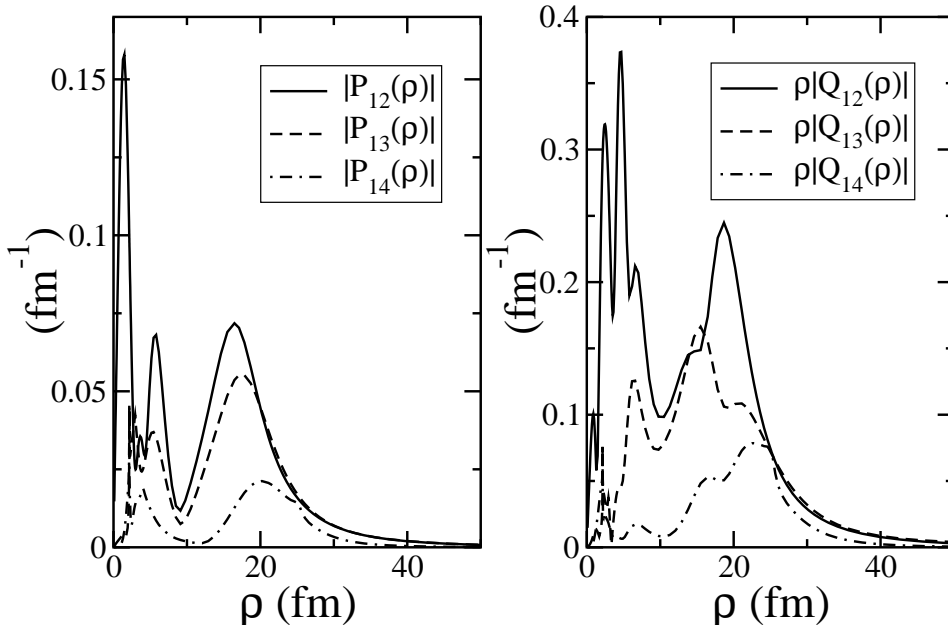


Fig. 3. The coupling potentials between the four dominating adiabatic levels for $\theta = 0.10$ rads shown as functions of ρ for ${}^6\text{He}(2^+)$. The first and the fourth levels have similar quantum numbers but approach the $K = 2$ and 4 levels, respectively. To show the first (P) and second (Q) order coupling potentials in the same units (fm^{-1}) we multiply Q by ρ . (The energy unit is restored in the coupling potentials by including the omitted factor, i.e. $\hbar^2 Q/(2m)$, $\hbar^2 P/(2m)\partial/\partial\rho$).

as matrix elements of first and second radial derivatives of the angular wave functions. Thus, radial couplings between rapidly changing angular structures are inevitable.

In Fig. 3 we show how the strongly varying coupling potentials can be related to the changing angular structure seen in Fig. 2. The peaks are most pronounced when a crossing is avoided and the two levels switch characteristics [16]. The rather confusing coupling picture is crucial for the asymptotic behavior of the wave function at large distance where the energy distribution is determined. The second order terms are substantially larger than the first order couplings but all vanish at large ρ . Thus the numerical computations in the present case must extend at least beyond $\rho \approx 40$ fm where the couplings have reached very small values. This is about two times the largest scattering length which defines the distance of convergence towards asymptotic values.

We have now established two important but competing effects, which determine the three-body resonance structure from small to large values of ρ . In the extreme, the structure can either remain unchanged by climbing correspond-

ingly up on the adiabatic potentials, or the structure can change to follow that of the lowest-lying adiabatic wave function. A compromise between following the energetically most favored configuration and the resistance to a change of structure therefore must be reached. The combination of these effects determine the relative population of the different components in the radial solution, which in turn determines the observable energy distribution. The couplings are more important here than for widths, energies and small-distance wave functions. They must be accurately computed to provide the energy distribution.

The structure of the resonance wave function at large ρ could remain unchanged and only exhibit a simple scaling behavior proportional to ρ . This is typical of direct decay. The wave function could also have large probability for finding two close-lying particles where the hyperradius mainly changes by moving the third particle as ρ increases. This is typical of sequential decay via more or less stable two-body configuration, e.g. sequential decay through two-body resonances. The intermediate configuration does not necessarily need a confining barrier, but could be provided by low-lying two-body virtual s -states [21]. Mixtures of all types can occur giving rise to the description of decay properties as fractions proceeding via individual two-body configurations. All these structures can be computed by use of our method, although convergence for the Coulomb interaction is more difficult.

The best strategy to get reliable results is not obvious, because the brute force method of increasing basis size and hyperradius until convergence is reached may be beyond any reasonable computer effort. The indecision is related to the requirement of an increasing basis with increasing ρ , which means that a smaller ρ and a smaller basis could provide a better description with much less effort. In other words a convergence may be reached in a region of ρ -values for a moderate basis size. This convergence would be destroyed as ρ is allowed to increase because the basis size cannot follow. The convergence can possibly be reached faster by extrapolation of the observable distribution by use of a known or anticipated dependence of ρ and basis size [31]. Different parts of the wave function may extrapolate differently. The most efficient choice depends on the (mixtures of) decay mechanisms which therefore has to be determined first. Therefore the first step is to compute the structure of the resonance wave functions as discussed in [20].

4 Realistic numerical illustration: ${}^6\text{He}(2^+)$

Nuclear three-body decay without complications of the Coulomb interaction must involve emission of two neutrons. The decaying states do not have to be three-body structures although such two-neutron halos are available and rather well studied. The most obvious case is the established 2^+ resonance in

${}^6\text{He}$ which is formed by the same neutron-core components as in the ground state.

Without Coulomb interactions the computations should quickly lead to the desired energy distributions. However, even short-range interactions can present difficulties as highlighted by the intricate description needed for the Efimov effect [16]. Both the α -neutron and the neutron-neutron interactions are previously employed in ground state computations [16].

We follow the procedure outlined in the preceding sections. Different prescriptions are possible to implement the Pauli principle [32], all of them providing indistinguishable angular wave functions at large distances. We adjust the three-body potential to give the correct resonance energy. This only requires marginal fine-tuning. In total 1132 hyper-spherical harmonics are used in the expansion (21), and the maximum value of K is 200 for the most relevant partial wave components and never smaller than 40. The resonance wave function is then available as function of the hyperspherical coordinates. A complex scaling angle of 0.10 rads is enough to produce an exponentially vanishing with increasing ρ wave function for the resonance. A different scaling angle, where the numerical calculations have converged, produce the same results.

4.1 Resonance structure

We already showed the angular eigenvalues and the adiabatic potentials in Fig. 1. The probability distribution arising from only the lowest potential was shown in [20]. The structure changes from peaks at small ρ corresponding to α -neutron $p_{3/2}$ -structure to a probability with one broad peak corresponding to comparable distances between all three particles. This reflects the change of structure of this angular wave function from small to large ρ as seen in details in Fig. 2. Eventually the lowest hyperharmonic function with $K = 2$ is approached. This indicates in itself a direct decay mechanism. However, in this case the lowest potential provides rather misleading results.

The rapidly changing structure seen in Fig. 2 at around $\rho \approx 20$ fm could easily lead to occupation of higher-lying levels. These occupation probabilities are functions of ρ and simply found as squares of the radial wave function obtained by solving the coupled set of radial equations. The results are shown in Fig. 4 for the lowest adiabatic components. At small ρ the lowest potential is totally dominating but as ρ increases the lowest three components contribute with comparable amplitudes. All radial wave functions vanish by oscillating around zero with decreasing amplitudes. The relative sizes are more clearly seen in the right hand side of Fig. 4. After the transition around 20 fm the individually very small radial amplitudes stabilize on relatively constant finite

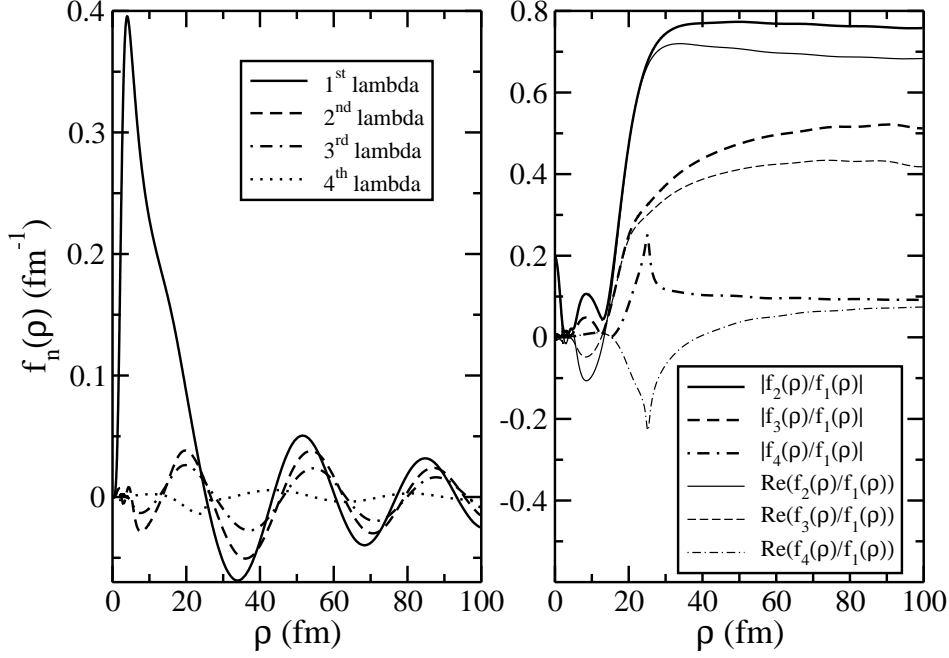


Fig. 4. The radial wave functions (left) and the absolute values and real parts of their relative sizes (right) corresponding to the four dominating adiabatic potentials for $\theta = 0.10$ rads as functions ρ for the ${}^6\text{He}(2^+)$ resonance.

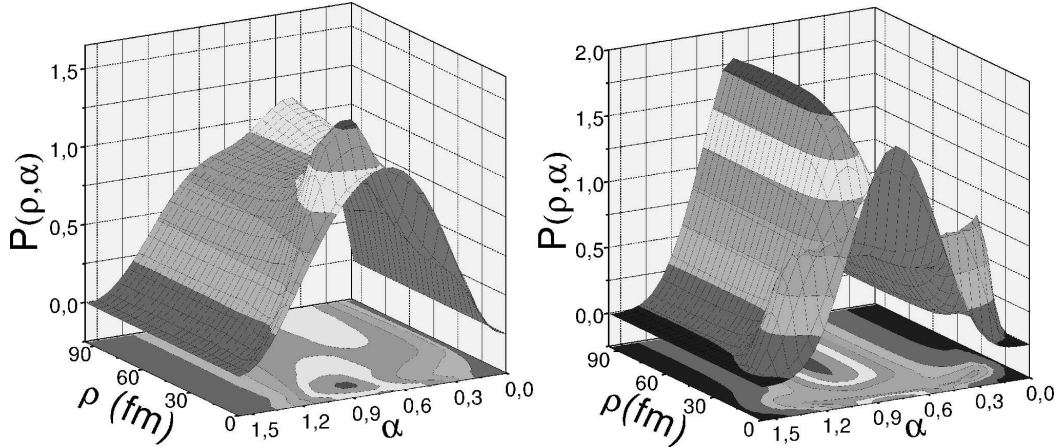


Fig. 5. The probability distribution for ${}^6\text{He}(2^+)$ including the lowest 8 adiabatic potentials as function of hyperradius ρ and hyperangle α related to the distance by $r_{ik} \propto \rho \sin \alpha$, i.e. the distance between either the one neutron and core r_{nc} (left) or the two neutrons r_{nn} (right).

ratios. The square of these give the relative weights, i.e. reduced compared to the first component by about 0.6, 0.25, 0.01 for the second, third and fourth potential, respectively. The transition to stable ratios is consistent with the disappearance of the coupling terms shown in Fig. 3.

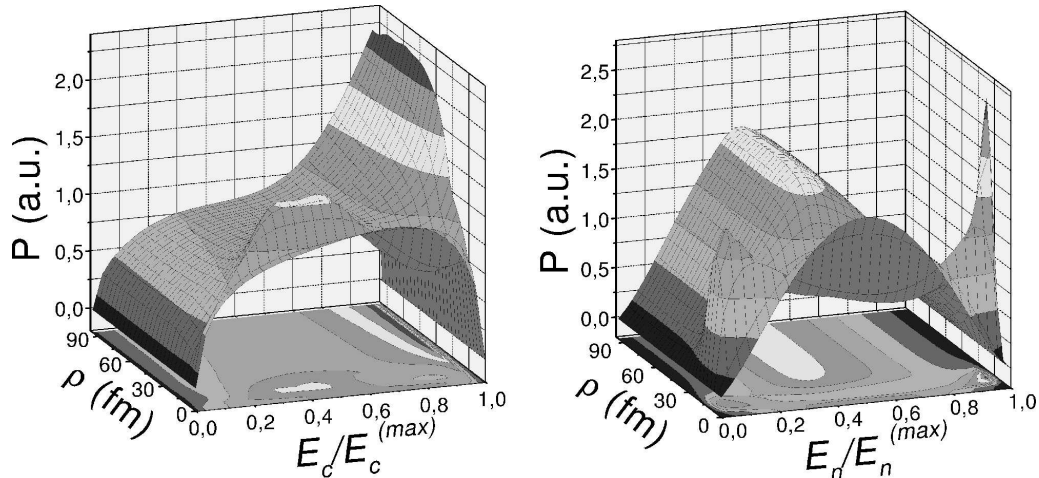


Fig. 6. The energy distributions of neutrons (right) and α -particles (left) after decay of ${}^6\text{He}(2^+)$ for $\theta = 0.10$ rads. The three-dimensional plot show the dependence on ρ with inclusion of 8 adiabatic wave functions. The maximum energies are $(m_\alpha + m_n)/(m_\alpha + 2m_n)E_0$ and $2m_n/(m_\alpha + 2m_n)E_0$ for the neutron and the α -particle, respectively. Here E_0 is the energy of the decaying resonance.

The total probability distribution in Fig. 5 are quite different from that of the lowest eigenvalue. At large ρ the probability now peaks at a smaller distance between the two neutrons and correspondingly the α -neutron distance is increased. Still fairly broad distributions remain. The decay mechanism indicated by this structure is now instead of direct rather a mixture between the preferred sequential decay via a neutron-neutron intermediate configuration and a smaller direct component.

4.2 Energy distributions

Reliable computation of the energy distribution requires numerically converged results in an appropriate region of ρ -values. The energy distributions are shown in Fig. 6 as functions of ρ for a sufficiently large number of adiabatic potentials. The resemblance with the probability distribution is not surprising since only the volume element has been changed. The observable distribution is the cut for constant, and sufficiently large, ρ where convergence has been reached as function of basis size. The neutron energy distribution has two peaks for small ρ corresponding to the geometric configurations of one neutron close to the α -particle and the other neutron further away. This is reflected in the peak in the α -spectrum at intermediate energies corresponding to the same geometric configurations.

The structure changes with ρ into a broad peak at intermediate energies for the neutron spectrum, and one peak very close to the maximum energy for the α -spectrum. This is the fingerprint of sequential decay via emission of the α -particle followed by decay of an intermediate two-neutron structure. This is easily visualized as the two-body decay process where the α -particle receives

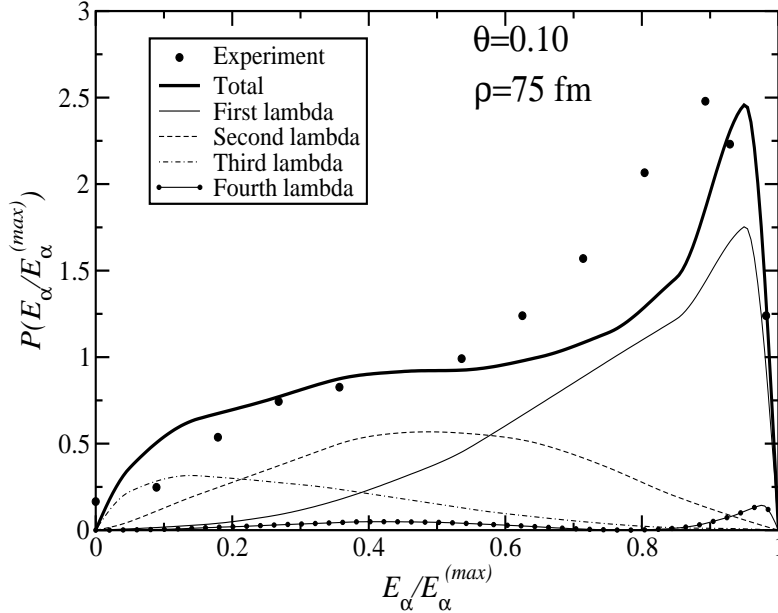


Fig. 7. The energy distribution of the α -particle after decay of the 2^+ -resonance in ${}^6\text{He}$. The scaling angle is $\theta = 0.10$ rads and $\rho = 75$ fm where convergence is reached. The points are extracted from the measurements in [4]. Contributions from the 4 dominating adiabatic potentials are shown individually.

maximum energy when the two neutrons move together in the opposite direction. In the subsequent decay each neutron then must share the remaining energy which leads to an intermediate energy between zero and the maximum value.

This inferred decay mechanism is perhaps counter-intuitive because stable intermediate configuration of two neutrons do not exist neither as bound states nor as resonances. It would be much more acceptable with the α -neutron $p_{3/2}$ -resonance as the intermediate structure. However, one characteristic feature of the neutron-neutron interaction is the low-lying virtual s -state which simply means that there is a substantial s -wave attraction. Apparently this is decisive for the decay process where the two neutrons end up by moving essentially in the same direction, and then necessarily guided by the attraction. The interesting point is maybe that this is not the way they started out at small distance in the spatially confined part of the wave function. This change of structure with hyperradius is in a sense reflecting the dynamic character of the decay process. At distances larger than the scattering length the short-range interactions are negligibly small, the wave function changes are completed and the asymptotics are established.

The microscopic structure of the energy distributions can be studied by dividing into contributions from the individual adiabatic potentials as seen in Fig. 7 for the emitted α -particle. The total distribution remains essentially unchanged if more than the four dominating potentials are included. Each

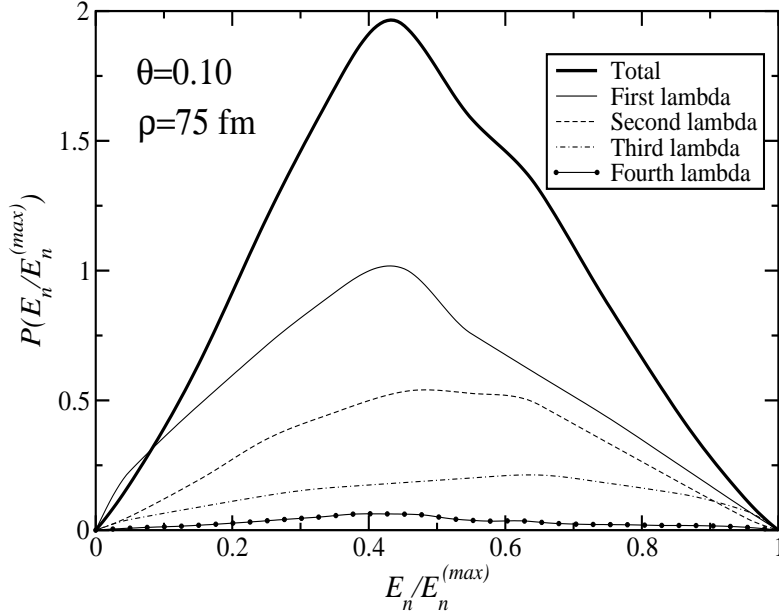


Fig. 8. The same as Fig. 7 for the neutrons emerging after decay of the 2^+ -resonance in ${}^6\text{He}$.

contribution has its own characteristic feature. The first has a peak close to the maximum energy, i.e. resembling α -emission from a neutron-neutron 0^+ -state. The second has a peak at intermediate energy, i.e. resembling sequential decay by the α -neutron resonance. The third has a peak at small energy, i.e. resembling α -emission from an excited neutron-neutron 2^+ -state. In addition the fourth potential also gives a small contribution with maxima at intermediate and maximum energy. The size of about 1% cannot be seen in the total distribution. However, this eigenvalue has the same angular momentum quantum numbers as the first level. Therefore the non-diagonal interference term would be about 10% of the total contribution. It turns out that the interference essentially is destructive and responsible for the almost flat region at intermediate energies.

The decay mechanism is then not simple although understandable in terms of our formulation. The main contribution is decay via the virtual s -state and the second is from direct decay. The third mechanism is produced by the coupling to the higher-lying state taking place at relatively small ρ . This populates the level eventually approaching the $K = 4$ hyperspherical level at large ρ . The interference with the dominating contribution then leads to the total distribution. The division into these different contributions of direct and sequential is to some extent artificial but perhaps useful in connection with the experimental analysis.

The mixture of all these contributions leads to the total distribution which has the right features but without precise reproduction of the high-energy peak, see Fig. 7. Experimental resolution would not improve very much because ei-

ther the peak gets broader and lower, or it gets higher and narrower. The discrepancies can originate from the presence of the target and the reaction mechanism itself as well as from contributions to the experimental points from other than resonance decays. The experiment selects the window of energies around the 2^+ resonance position in the reaction ${}^7\text{Li}({}^2\text{H}, {}^3\text{He}){}^6\text{He}^*$. This necessarily includes some background which perhaps has a different energy distribution than the 2^+ resonance we investigated in the present calculations. We find a distribution where the two-neutron virtual s -state dominates whereas the measurements are broader as expected from non-resonance decays. In this work we focus on the decay of "populated" resonances, and an appropriate description of this reaction goes beyond the scope of the paper.

An attempt to understand the distribution was published soon after the experiment in [4]. The measured distribution was fitted by a linear combination of the lowest hyperharmonic functions of $K = 2$ and 4. The conclusion was that a substantial $K = 4$ component is needed to reproduce the experiment. The decay mechanism dominated by the neutron-neutron virtual s -state was abandoned in favor of the $K = 4$ component. This phenomenological analysis provides a good fit even for energies above the maximum allowed by the resonance energy. The decaying resonance wave function does not enter anywhere. The significance is not easy to interpret in terms of decay mechanisms as attempted in the present work.

The neutron energy distribution is not measured but for future comparison we show our prediction in Fig. 8. The division into different adiabatic components show that the broad total distribution centered around an intermediate energy is obtained by adding several qualitatively similar contributions. The different mechanisms would all produce most likely energies around half the maximum value. To distinguish it is therefore necessary to measure both α -particles and neutrons after the decay.

4.3 *Dependence on scaling angle*

It is instructive to investigate the dependence of the distributions on the choices of ρ , θ and basis size. The ρ -dependence is already indicated in Fig. 6 where the distributions are very stable as soon as ρ is larger than about 50 fm. However, this stability does require a sufficiently large basis which at least up to 100 fm still can be handled in modest-size computers. It is also clear that a finite basis cannot accurately describe the solutions when ρ increases towards ∞ . Then the angular solutions approach the hyperharmonics but a large basis is still required to reproduce the structures at small distances between pairs of particles. Eventually this becomes impossible. The many basis functions cancel each other at larger distances.

At intermediate distances, where the basis is sufficiently large, the resonance wave functions are independent of ρ . For the radial solution this is seen in the right part of Fig. 4, where for ρ larger than about 50 fm, the ratio between the different radial components is approximately constant. The energy distributions are mainly dominated by the absolute squares of these ratios, although when different adiabatic components interfere also the real parts of these complex ratios may contribute individually. This behavior of the radial ratios is responsible for the stable behaviour of the energy distributions for sufficiently large values of ρ . The constant behavior of the radial ratios also implies that the radial wave functions have already reached asymptotics as given in eq.(22) for all the channels, and therefore the distributions are independent of the scaling angle. However, the latter conclusion is based on an assumption of analyticity of the angular solutions as function of θ . When this scaling angle is changed corresponding to a rotation across a singularity like a two- or three-body resonance the continuity is broken and the solutions change as well.

This is especially clear when we compare two solutions with θ smaller and larger than the angle corresponding to a two-body resonance. For the large θ one angular eigenvalue changes character and increases towards infinity as ρ^2 , see [26]. This qualitative change of behavior necessarily causes a change of the angular wave functions because the upgoing eigenvalue at large distances fully describes the properties of the two-body resonance. These features were distributed over several wave functions for the small θ -value.

In between singularities the individual angular solutions are independent of both ρ and θ . This may not be an apparent feature of the numerical solutions because the basis has to be sufficiently large for a complete description. As θ increases the effective ranges of the two-body interactions also increase and the stable region is pushed to larger ρ -values. This means that the minimum basis size has to increase with θ .

5 Summary and conclusions

We formulate a method to compute the energy distribution of three particles emerging after three-body decay of a many-body resonance. The complex energy of a resonance corresponds to a pole in the momentum-space wave function which has an absolute square of the form as Breit-Wigner shape multiplied by a smoothly varying function. In coordinate-space this form corresponds to a large-distance asymptotic wave function consisting of only outgoing waves. We show formally by Fourier transformation that the coordinate-space asymptotic angular dependence determines the energy distribution by substituting momentum directions for the conjugate coordinate directions. For this the

divergent Fourier integral is regularized by the Zeldovich prescription.

For two-body decay the energy distribution is trivially given by the Breit-Wigner distribution of the initial resonance. Energy conservation is taking care of everything else. For three-body decay the total energy can be distributed continuously among the three particles. We show that the resonance decay results in distributions obtained from the large-distance angular behavior of the coordinate wave function. The asymptotic behavior can correspond to either genuine three-body structures or two-body substructures for example corresponding to two-body resonances or configurations favored by substantial attraction as for virtual states. Also virtual population of two-body intermediate substructures is allowed as an appropriate asymptotic behavior with a resulting special energy distribution. The different asymptotics characterize the different decay modes used in analyses of experimental data. Different modes can co-exist.

We illustrate by the decay of the 2^+ -state in ${}^6\text{He}$. The practical computations employ the hyperspherical adiabatic expansion combined with the complex scaling method. We discuss how a large hyperradius necessarily must be accompanied by a large basis. Convergent results may then be obtained with less efforts at moderate hyperradii and moderate basis sizes. For convergence it is crucial to have all three Faddeev components, and especially if all decay mechanisms simultaneously should be included in the theoretical formulation. The wave function undergoes dramatic changes from small distances, where the resonance properties usually are determined, and large distances from which the energy distributions emerge. The reasons for these structural changes are that the small distance behavior is determined by the two-body resonance substructures, whereas the large-distance behavior is determined as a competition between two effects, i.e. the energetically favored configuration of smallest two-body angular momentum with attractive two-body potentials and maintaining the same structure as at small distances in higher-lying levels.

In conclusion, theoretical interpretation of the simplest nuclear three-body decay without Coulomb interactions is already rather complicated. It is then advisable to test any given method on these systems. The accuracy of computations of the more complicated decaying charged systems can then be judged. This is important since almost all nuclear three-body resonance decays involve charged systems. The goal is to interpret the soon-to-come accurate experimental correlation data for three-body decays of charged systems.

References

- [1] P.J. Siemens and A.S. Jensen, Elements of nuclei. Many-body physics with the strong interaction, Addison-Wesley, California 1987.
- [2] A.S. Jensen, K. Riisager, D.V. Fedorov and E. Garrido, Rev. Mod. Phys. **76** (2004) 215.
- [3] W. Glöckle H. Witala, D. Hüber, H. Kamada and J. Golak, Phys. Rep. **274** (1996) 107.
- [4] B.V. Danilin, M.V. Zhukov, A.A. Korshennikov, L.V. Chulkov V.D. Efros, Sov. J. Nucl. Phys. **46** (1987) 225.
- [5] O.V. Bochkarev et al., Nucl. Phys. **A505** (1989) 215.
- [6] R.J. Kryger et al., Phys. Rev. Lett. **74** (1995) 860.
- [7] C.R. Bain et al., Phys. Lett. **B373** (1996) 35.
- [8] Gomez del Campo et al., Phys. Rev. Lett. **86** (2001) 43.
- [9] J. Giovinazzo et. al., Phys. Rev. Lett. **89** (2002) 102501.
- [10] M. Pfützner et al., Eur. Phys. J. **A14** (2002) 279.
- [11] M. J. Chromik et al., Phys. Rev. **C66** (2002) 24313.
- [12] H.O.U. Fynbo et al., Phys. Rev. Lett. **91** (2003) 82502.
- [13] B. Blank, J. Giovinazzo and M. Pfützner, *C.R. Physiques* **4**, (2003).
- [14] T. Zerguerras et al., Eur. Phys. J. **A20** (2004) 389.
- [15] B. Blank et al., Phys. Rev. Lett. **94** (2005) 232501.
- [16] E. Nielsen, D.V. Fedorov, A.S. Jensen and E. Garrido, Phys. Rep. **347** (2001) 373.
- [17] D. V. Fedorov, A. S. Jensen and H.O.U. Fynbo, Nucl. Phys. **A718** (2003) 685c.
- [18] E. Garrido, D.V. Fedorov, A.S. Jensen and H.O.U. Fynbo, Nucl. Phys. **A748** (2005) 27.
- [19] O.I. Kartavtsev, Few-Body Systems **34** (2004) 39.
- [20] E. Garrido, D.V. Fedorov, A.S. Jensen and H.O.U. Fynbo, Nucl. Phys. **A748** (2005) 39.
- [21] E. Garrido, D.V. Fedorov and A.S. Jensen, submitted for publication.
- [22] D.V. Fedorov, H.O.U. Fynbo, E. Garrido and A.S. Jensen, Few-body systems **34** (2004) 33.
- [23] Ya..B. Zeldovich, Sov.Phys. JETP **12** (1961) 542.

- [24] R.G. Newton, Scattering theory of waves and particles, Springer-Verlag, New York 1982..
- [25] S.Yu. Ovchinnikov, G.N. Ogurtsov, J.H. Macek, Yu.S. Gordeev, Phys. Rep. **389** (2004) 119.
- [26] D.V. Fedorov, E. Garrido, and A.S. Jensen, Few-body systems, **33** (2003) 153.
- [27] H. Kameyama, M. Kamimura and Y. Fukushima, Phys. Rev. **C40** (1989) 974.
- [28] D.V. Fedorov, A. Cobis and A.S. Jensen, Phys. Rev. **C59** (1999) 554.
- [29] D. V. Fedorov and A. S. Jensen, Phys. Lett. **B389** (1996) 631.
- [30] V.M. Efimov, Phys. Lett. **B33** (1970) 563.
- [31] T. N. Rescigno, M. Baertschy, W. A. Isaacs, C. W. McCurdy, Science, **286** (1999) 2474.
- [32] E. Garrido, D.V. Fedorov and A.S. Jensen, Nucl. Phys. **A650** (1999) 247.